frontiers | Frontiers in Marine Science

TYPE Original Research
PUBLISHED 09 November 2022
DOI 10.3389/fmars.2022.1030519

OPEN ACCESS

EDITED BY
Adriana Vallesi,
University of Camerino, Italy

REVIEWED BY
Xiangrui Chen,
Ningbo University, China
Peter Vdacny,
Comenius University, Slovakia

*CORRESPONDENCE
Xiaofeng Lin
linxf@xmu.edu.cn

SPECIALTY SECTION
This article was submitted to Marine Evolutionary Biology, Biogeography and Species Diversity, a section of the journal Frontiers in Marine Science

RECEIVED 29 August 2022
ACCEPTED 12 October 2022
PUBLISHED 09 November 2022

CITATION
Zhang Y, Yu Y, Qu Z, Jiang M, Shen Z, Li J and Lin X (2022) Taxonomy and phylogeny of *Pseudovorticella* ciliates (Ciliophora, Peritrichia): Two new and one rare species from the coastal waters of China.
Front. Mar. Sci. 9:1030519.
doi: 10.3389/fmars.2022.1030519

Taxonomy and phylogeny of *Pseudovorticella* ciliates (Ciliophora, Peritrichia): Two new and one rare species from the coastal waters of China

Yong Zhang[1], Ying Yu[1], Zhishuai Qu[1,2], Mengmeng Jiang[3], Zhuo Shen[4], Jiqiu Li[1,2] and Xiaofeng Lin[1,2]*

[1]Key Laboratory of Ministry of Education for Coastal and Wetland Ecosystems, Fujian Provincial Key Laboratory of Coastal Ecology and Environmental Studies, College of the Environment and Ecology, Xiamen University, Xiamen, China, [2]State Key Laboratory of Marine Environmental Science, Xiamen University, Xiamen, China, [3]School of Life Science, South China Normal University, Guangzhou, China, [4]Laboratory of Microbial Ecology and Matter Cycle, School of Marine Sciences, Sun Yat-sen University, Zhuhai, China

Peritrich ciliates are a species-rich group of sessile unicellular eukaryotes, which can be found in various aquatic habitats from all over the world. It is well accepted that there are still many ciliates to be uncovered. During a survey on ciliate biodiversity in the coastal waters of China, three solitary peritrich species were identified as members of the genus *Pseudovorticella* Foissner & Schiffmann, 1975, including two new species and a rare one. *Pseudovorticella zhejiangensis* sp. n. differs from its congeners mainly by having a conical-shaped zooid, conspicuous pellicular blisters, one ventral and one dorsal contractile vacuoles, and an infundibular polykinety 3 with three rows of nearly equal length but different beginning positions. *Pseudovorticella dalianensis* sp. n. can be defined mainly by an obovoid-shaped zooid, one ventral contractile vacuole, and a three-rowed infundibular polykinety 3 with the middle row being the longest. The rare species, *Pseudovorticella verrucosa* (Dons, 1915) Sun et al., 2009, was redescribed. The small subunit (SSU) rDNA sequences of these three species were sequenced for the first time, the phylogeny of *Pseudovorticella* species was analyzed, and the results verified the non-monophyly of this genus. This study demonstrates that the morphologic and gene barcoding data are the optimum combination to disclose the biodiversity of ciliates.

KEYWORDS

biodiversity, morphology, molecular phylogeny, sessile ciliates, SSU rDNA

Introduction

Sessile peritrich ciliates comprise over 800 species and can be commonly found in a wide variety of aquatic habitats including marine, freshwater, and brackish waters (Jankowski, 1985; Song, 1991; Foissner et al., 1992; Berger and Foissner, 2003; Sun et al., 2016; Wu et al., 2020; Wu et al., 2021). These ciliates are highly sensitive to environmental changes, thus are frequently used as bioindicators for water quality assessment (Xu et al., 2014) and the assessment of sludge activity in wastewater treatment plants (Foissner, 2016). However, it has long been recognized that many peritrich species are often difficult to identify, especially for two species-rich genera, *Pseudovorticella* Foissner & Schiffmann, 1975 and *Vorticella* Linnaeus, 1767 (Ji et al., 2004; Sun et al., 2013). The species of the two genera are difficult to distinguish only by living morphology. The only difference is that *Pseudovorticella* has a reticulate silverline system while *Vorticella* has a transverse pattern (Foissner and Schiffmann, 1975).

Up to date, over 60 *Pseudovorticella* species have been identified (Zhang et al., 2019), most of which were transferred from *Vorticella* (Foissner and Schiffmann, 1975; Foissner and Schiffmann, 1979; Leitner and Foissner, 1997; Sun et al., 2009; Ji et al., 2011; Gómez et al., 2018; Hu et al., 2019). The lack of silver staining information, especially the pattern of the silverline system of many *Vorticella* species, still questions their generic assignments and, thus, gives rise to the challenge in the identification of *Pseudovorticella* ciliates (Noland and Finley, 1931; Warren, 1986; Warren, 1987; Sun et al., 2013; Liang et al., 2019). Molecular studies based on gene sequence data can serve as a supplementary tool to species identification and can help reveal the phylogenetic relationships among peritrich ciliates (Clamp, 2006; Zhan et al., 2009; Chen et al., 2010; Foissner et al., 2010; Ji et al., 2011; Gao et al., 2016; Sun et al., 2016). However, so far, there are only about 34 available small subunit (SSU) rDNA sequences of *Pseudovorticella* isolates in the public databases, covering 11 known species. Therefore, both the species diversity and the genetic variation of this genus have not yet been well revealed (Sun et al., 2013; Jiang et al., 2019).

As a contribution to the species diversity of *Pseudovorticella*, two new species and one known species were isolated during a survey on ciliate diversity in the coastal waters of China. They were studied in detail using state-of-the-art taxonomic methods of ciliates. The morphological information including live morphology, ciliature patterns, and silverline systems was documented. In addition, the SSU rDNA sequences were also provided and used to conduct phylogenetic analyses.

Materials and methods

Sample collection and cultivation

Pseudovorticella zhejiangensis sp. n. was collected on 11 March 2017 from a coastal pond in Taizhou, Zhejiang Province, China (28°14′18.80′′N, 121°14′16.33′′E). *Pseudovorticella dalianensis* sp. n. was collected on 21 July 2017 from a coastal water in Dalian, Liaoning Province, China (38°52′2.92′′N, 121°33′56.06′′E). *Pseudovorticella verrucosa* (Dons, 1915) Sun et al., 2009 was collected on 16 December 2009 from the Clear Water Bay, Hong Kong, China (22°16′53.54′′N, 114°19′4.51′′E). After collection, samples were transferred into Petri dishes and cultivated at room temperature (20°C–25°C) for several days; rice grains were added to enrich bacteria as a food source for ciliates.

Live observation and silver staining

During the lab cultivation, living cells were observed using bright field and differential interference contrast microscopy (Nikon 80i, Tokyo, Japan). The ciliature pattern and nuclear apparatus were revealed by the protargol staining method following Wilbert (1975). The Chatton–Lwoff silver nitrate staining method according to Song and Wilbert (1995) was conducted to show the silverline system. Drawings of live specimens were based on *in-vivo* observations and photomicrographs at ×100–1,000 magnifications, and those of stained specimens were performed with the aid of a camera lucida at a magnification of ×1,000. Morphometric measurement of the stained specimens was conducted at a magnification of ×1,000. Systematics and terminology were mainly according to Warren (1987) and Lynn (2008).

DNA extraction and SSU rDNA sequencing

For each species, about 10 individuals were transferred from the Petri dishes to watch glass plates, washed carefully three times, and filtered (through 0.2-μm membranes) in site water. Then, a single individual was harvested and placed in a 1.5-ml centrifuge tube prior to DNA extraction. Several backups were made for each species. Genomic DNA was extracted using RED Extract-N-Amp Tissue PCR Kit (Sigma, USA) following the default procedure. The SSU rDNA sequence was amplified by PCR, using the universal eukaryotic forward primer EukA (5′-AACCTGGTTGATCCTGCCAGT-3′) and reverse primer EukB (5′-TGATCCTTCTGCAGGTTCACCTAC-3′) (Medlin et al., 1988). The PCR setting parameters were as follows: an initial denaturation at 98°C for 3 min, 35 cycles for amplification (15 s at 98°C, 15 s at 54°C, and 90 s at 72°C), and a final extension at 72°C for 10 min. The PCR products were checked and sent for sequencing. The SSU rDNA was sequenced by Shanghai Majorbio Bio-Pharm Technology Co., Ltd. (Guangzhou branch), and near full-length sequences of the three species were obtained.

Phylogenetic analyses

Including the three newly obtained sequences, 75 SSU rDNA sequences (NCBI accession numbers shown in Figure 7) were

used for phylogenetic analyses. Sequences were aligned using the in-built ClustalW function in BioEdit 7.2.5 (Hall, 1999), then further modified by the truncation of both ends and the removal of ambiguous positions. The length of the final aligned matrix was 1,462 bp. This matrix was used to construct phylogenetic trees (Supplementary Materials S1, S2). Two hymenostomes, *Tetrahymena corlissi* (U17356) and *Glaucoma chattoni* (X56533), served as outgroup taxa.

Three algorithms were employed to construct the phylogenetic trees. A maximum likelihood (ML) analysis was run using the RAxML-HPC2 v. 8.2.12 package (Stamatakis, 2014) on the CIPRES website (Miller et al., 2010) with the GTRGAMMA + I nucleotide substitution model (Irwin and Lynn, 2015); 1,000 bootstrap replicates were conducted (Supplementary Material S3). Another ML analysis was run using IQ-TREE multicore version 1.6.12 (Minh et al., 2020) (Supplementary Material S4). The model TIM2+F+R5 was chosen as the best-fit model according to the Bayesian information criterion (BIC) by the in-built ModelFinder program (Supplementary Material S5). Statistical support was computed using 1,000 ultrafast bootstrap replicates (Hoang et al., 2018). A Bayesian inference (BI) analysis was run using MrBayes on the XSEDE 3.2.7a package (Ronquist and Huelsenbeck, 2003) on the CIPRES website (Supplementary Materials S6, S7). The best-fit model TIM2+I+G was determined according to BIC, using the jModeltest 2.1.10 package (Darriba et al., 2012) on the CIPRES website (Supplementary Material S8). The model parameters were added to the command blocks for the construction of BI trees (Supplementary Material S2). The Markov chain Monte Carlo simulations were run for four million generations. The sample frequency was every 100th generation, and the first one million simulations were discarded as burn-in. The average standard deviation of split frequencies was 0.005859 (<0.01).

The pairwise genetic distances among 25 *Pseudovorticella* SSU rDNA sequences were calculated with MEGA7.

Nomenclatural note

This work was registered in ZooBank under the following accession number: urn:lsid:zoobank.org:pub:78C7FC86-C1FF-4666-86B2-A764ADAA8F14.

Results

Taxonomy and morphological descriptions

Order Sessilida Kahl, 1933
Family Vorticellidae Ehrenberg, 1838
Genus *Pseudovorticella* Foissner & Schiffmann, 1975

***Pseudovorticella zhejiangensis* sp. n.**

Diagnosis. Zooid shape conical to elongated conical, about 50–70 × 45–70 μm *in vivo*. Macronucleus J-shaped. Two contractile vacuoles, one ventral and the other dorsal. Pellicle with pellicular blisters. Infundibular polykinety 3 with three rows of nearly equal length, the beginning position of the inner row different from that of the outer two rows. 31–38 and 9–17 transverse silverlines above and below the aboral trochal band, respectively.

Type locality. A coastal pond in Taizhou, Zhejiang Province, China (28°14′18.80′′N, 121°14′16.33′′E). Water temperature was 18°C, salinity was 15‰, and pH was 7.

Type materials. A permanent slide (registration number: JMM-2017031101) with protargol-impregnated specimens of which the holotype was circled in black and a slide (registration number: JMM-2017031102) with silver nitrate-stained specimens as paratype were deposited in the Laboratory of Protozoology, Ocean University of China, Qingdao, China.

Etymology. The group name *zhejiangensis* refers to the location, Zhejiang Province, China, where the type was found.

ZooBank accession number of the new species. urn:lsid:zoobank.org:act:715CCF74-9457-4F33-ABEF-19213CC252B6

Morphological description (Figures 1, 2 *and* Table 1)**.** Zooid 50–70 × 45–70 μm *in vivo* (Table 1), conical to elongated conical shaped, widest part at peristome (Figures 1A, E, 2A, I). Peristomial lip single-layered, about 5 μm thick. Peristomial disc flat, moderately elevated from the peristomial lip in fully extended cells (Figures 1A, 2B). Pellicle smooth at low magnifications, while irregularly shaped blisters and striations observed under magnifications of ×400 to ×1,000 (Figures 1A, B, 2C, D).

Cytoplasm dark to grayish, usually filled with small food vacuoles (1–2 μm across) and dark green algae-like particles (1–2 μm across) (Figure 2B). Two contractile vacuoles, each 4–8 μm in diameter; one located near the ventral wall of the infundibulum under the peristomial lip, the other dorsally located; contracting non-simultaneously with an interval of 1–1.5 min (Figures 1A, 2E). Macronucleus J-shaped (Figures 1A, 2F). Micronucleus not observed.

Stalk 217–345 μm in length *in vivo*, 5–8 μm in diameter, helically contractile; with no bacteria nor algae attached (Figures 1C, E, 2A, G, H). Stalk spasmoneme 2–3 μm across, distinctly helical, with black granules sparsely distributed on the surface (Figures 1C, 2G, H). Telotroch present.

Haplokinety and polykinety circles extending about 1.25 turns around the peristomial disc and another turn after entering the infundibulum (Figure 1G). Polykinety posteriorly separated into three infundibular polykineties (P1, P2, and P3) at the lower half of the infundibulum (Figure 1G). Each infundibular polykinety consisting of three rows (Figures 1G, 2J). P2 terminating at the confluence of P1 and P3. Three rows of P3 nearly equal in length; inner row beginning at the middle of the upper part of P2 and terminating at the same level as P2; outer

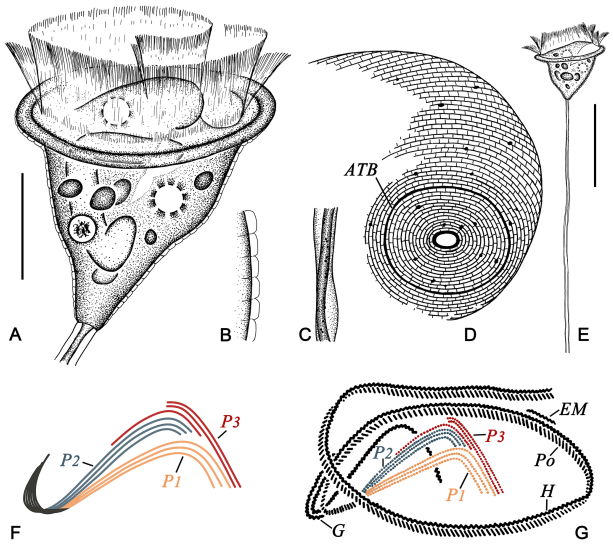

FIGURE 1
Pseudovorticella zhejiangensis sp. n. from life **(A–C, E)**, after silver nitrate staining **(D)**, and after protargol staining **(F, G)**. **(A)** Typical shape of the zooid. **(B)** Pellicular blisters. **(C)** Details of the stalk and spasmoneme. **(D)** Silverline system, showing the posterior part of the zooid. **(E)** An individual with stalk and zooid. **(F)** Arrangement pattern of the three infundibular polykineties. **(G)** Oral ciliature. ATB, aboral trochal band; EM, epistomial membrane; G, germinal kinety; H, haplokinety; Po, polykinety; P1–3, infundibular polykinety 1–3. Scale bars: 30 μm **(A)** and 60 μm **(E)**.

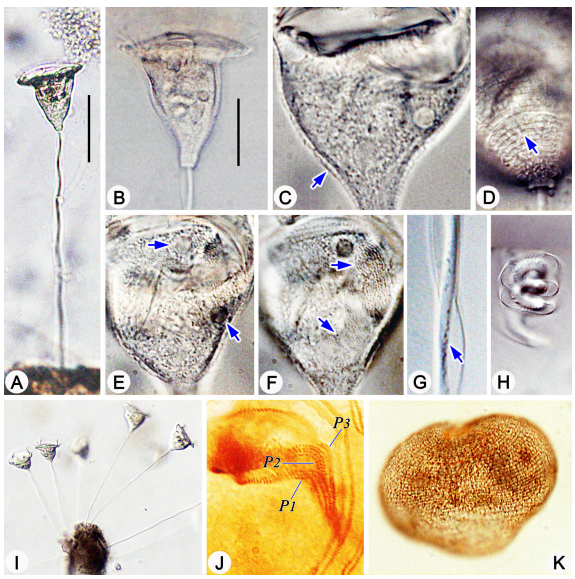

FIGURE 2
Photomicrographs of *Pseudovorticella zhejiangensis* sp. n. *in vivo* **(A–I)**, after protargol staining **(J)** and after silver nitrate staining **(K)**. **(A, I)** Typical complete individuals. **(B)** Zooid in typical shape. **(C)** Pellicular blisters (arrow). **(D)** Pellicular striations (arrow). **(E)** Macronucleus (arrows). **(F)** Arrows indicate the two contractile vacuoles, one dorsal and another ventral. **(G)** Details of the stalk and spasmoneme; arrow points to granules. **(H)** Helically contracted stalk. **(J)** Infundibular part of the oral ciliature, showing the three polykineties. **(K)** Overview of the silverline system. Abbreviations: P1–3, infundibular polykinety 1–3. Scale bars: 60 μm **(A)** and 30 μm **(B)**.

TABLE 1 Morphometric data of *Pseudovorticella zhejiangensis* sp. n., *Pseudovorticella dalianensis* sp. n., and *Pseudovorticella verrucosa*.

Character	Species	Min	Max	Mean	SD	*n*
Zooid length *in vivo* (μm)	*P. zhejiangensis*	50	70	58.3	6.26	12
	P. dalianensis	50	60	55.0	4.08	10
	P. verrucosa	30	50	41.3	5.93	10
Zooid width *in vivo* (μm)	*P. zhejiangensis*	45	70	59.6	7.97	10
	P. dalianensis	30	35	33.8	2.50	9
	P. verrucosa	50	65	52.6	4.55	10
Number of silverlines above the ATB	*P. zhejiangensis*	31	38	35.0	2.92	6
	P. dalianensis	31	44	38.0	4.19	7
	P. verrucosa	22	39	30.0	6.02	8
Number of silverlines below the ATB	*P. zhejiangensis*	9	17	12.0	2.73	8
	P. dalianensis	9	13	11.0	1.41	6
	P. verrucosa	13	20	16.8	2.62	8

ATB, aboral trochal band; Max, maximum; Mean, arithmetic mean; Min, minimum; SD, standard deviation; n, number of individuals measured.

two rows parallel, anterior parts separated from the inner row and terminating at the same level as P1 (Figures 1F, G, 2J). Germinal kinety located at the upper half of the infundibulum and parallel to haplokinety. Epistomial membrane located within the opening of the infundibulum (Figure 1G). Aboral trochal band composed of a row of kinetosomes encircling a cell at the posterior one-fifth of the body (Figure 1D).

Silverline system reticulate, with evenly spaced transverse lines (Figures 1D, 2K); 31–38 silverlines between the peristome and the trochal band, and 9–17 silverlines between the trochal band and the scopula (Table 1).

***Pseudovorticella dalianensis* sp. n.**

Diagnosis. Zooid obovoid-shaped, about 50–60 × 30–35 μm *in vivo*. Macronucleus J-shaped. One ventral contractile vacuole. Infundibular polykinety 3 with three rows, inner and outer rows shorter than the middle row and terminating near the end of P2; while the middle row terminating at the same level as P1; inner row clearly separated from the outer two rows and close to polykinety 2. 31–44 and 9–13 transverse silverlines above and below the aboral trochal band, respectively.

Type locality. Coastal marine water in Dalian, Liaoning Province, China (38°52′2.92′′N, 121°33′56.06′′E). Water temperature was 27°C, salinity was 30‰, and pH was 6.

Type materials. A permanent slide (registration number: JMM-2017072101) with protargol-impregnated specimens of which the holotype was circled in black and a slide (registration number: JMM-2017072102) with silver nitrate-stained specimens as paratype were deposited in the Laboratory of Protozoology, Ocean University of China, Qingdao, China.

Etymology. The group name *dalianensis* refers to the location, Dalian, where the type was found.

ZooBank accession number of the new species. Urn:lsid:zoobank.org:act:2EFAAB58-BDFE-4F9E-9A0B-2B9CFB36B9D9

*Morphological description (*Figures 3, 4 *and* Table 1*).* Zooid obovoid-shaped, 50–60 × 30–35 μm *in vivo* (Table 1). Single-layered peristomial lip about 5 μm thick, inconspicuously everted with uneven margin. Peristomial disc slightly elevated from the peristomial lip in fully extended cells (Figures 3A, 4B). Striations detectable under high magnifications of ×400 to ×1,000 (Figure 4H).

Cytoplasm dark to grayish, usually containing a few unequal-sized food vacuoles (5–8 μm in diameter) and dark green algae-like particles (3–5 μm in diameter) (Figures 3A, 4B). Single contractile vacuole about 10 μm in diameter, located near the ventral wall of the infundibulum (Figures 3A, 4C). Macronucleus J-shaped (Figures 3A, 4D). Micronucleus not observed.

Stalk 145–190 μm in length *in vivo*, about 3 μm in diameter, helically contractile; with no bacteria nor algae attached (Figures 3B, 4A, F, G). Stalk spasmoneme distinctly helical, 1–2 μm across, with granules sparsely distributed on the surface (Figures 3C, 4F). Telotroch not detected.

Haplokinety and polykinety extending about 1.25 turns around the peristomial disc and another turn after entering the infundibulum (Figures 3F, 4E). Polykinety posteriorly separated into three infundibular polykineties (P1, P2, and P3) at the lower half of the infundibulum (Figures 3F, 4E, I). Each infundibular polykinety consisting of three rows (Figures 3F, 4I). The middle row of P3 and P1 converged and synchronously terminating at the end of the infundibulum. P2 terminating at the confluence of P1 and P3. In P3, the inner and outer rows shorter than the middle row, and both terminating near the end of P2, while the middle row terminating at the same level as P1; inner row clearly separated from the outer two rows and close to P2 (Figures 3E, F, 4I). Germinal kinety located at the upper half of the infundibulum and parallel to haplokinety. Epistomial membrane positioned near the opening of the infundibulum (Figure 3F). Aboral trochal band composed of a row of kinetosomes encircling a cell at the posterior one-fifth of the body (Figures 3D, 4E).

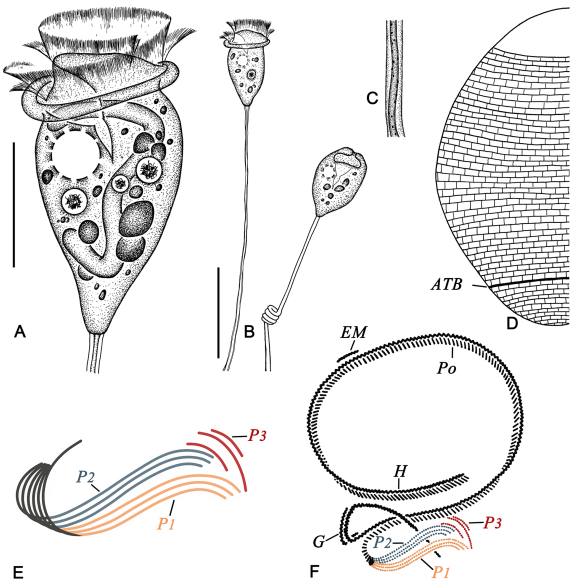

FIGURE 3
Pseudovorticella dalianensis sp. n. from life **(A–C)**, after silver nitrate staining **(D)** and after protargol staining **(E, F)**. **(A)** Typical shape of the zooid. **(B)** Complete individuals with stalk and zooid. **(C)** Details of the stalk and spasmoneme. **(D)** Silverline system. **(E)** Arrangement of the three infundibular polykineties. **(F)** Oral ciliature. ATB, aboral trochal band; EM, epistomial membrane; G, germinal kinety; H, haplokinety; Po, polykinety; P1–3, infundibular polykinety 1–3. Scale bars: 30 μm **(A)** and 60 μm **(B)**.

Silverline system reticulate, with evenly spaced transverse lines (Figures 3D, 4J). 31–44 and 9–13 transverse silverlines above and below the aboral trochal band, respectively.

***Pseudovorticella verrucosa* (Dons, 1915) Sun et al., 2009**

Improved diagnosis. Zooid inverted triangular-shaped, about 30–50 × 30–65 μm *in vivo*. Macronucleus J-shaped. Single contractile vacuole ventrally located. Pellicle with pellicular blisters and highly developed pellicular granules. Infundibular polykinety 3 with three rows, the inner row shorter than the outer two which are of equal length. 22–39 and 13–21 transverse silverlines above and below the aboral trochal band, respectively.

Deposition of voucher materials. A protargol-impregnated slide (registration number: SZ-2009-1216-02-1) and a silver nitrate-stained slide (registration number: SZ-2009-1216-02-03) with voucher specimens were deposited in the Laboratory of Protozoology, Ocean University of China, Qingdao, China.

Morphological description (Figures 5, 6 *and* Table 1)**.** Zooid inverted triangular-shaped, widest part at the peristome; cells size 30–50 × 50–65 μm *in vivo* (Table 1). Single-layered peristomial lip, about 4 μm thick, distinctly everted. Peristomial disc flat, slightly elevated above the peristomial lip in fully extended cells (Figures 5A, 6B). Pellicle with conspicuous blisters (about 2 μm thick) and sparsely distributed granules (1–3 μm diameter) (Figures 5A, D, 6E, G).

Cytoplasm grayish, usually containing several food vacuoles (3–5 μm across) (Figure 6B). One contractile vacuole situated near the ventral wall of the infundibulum, about 10 μm in diameter (Figures 5A, 6F). Macronucleus J-shaped; its upper arm horizontally oriented, surrounding the infundibulum almost completely; posterior portion extending to the posterior end of zooid (Figures 5H, 6H, I). Micronucleus not observed.

Stalk 300–400 μm in length *in vivo*, about 5 μm in diameter, helically contractile; occasionally with attachments on the surface (Figures 5C, 6A, C, D). Stalk spasmoneme about 3 μm across, distinctly helical, without granules on the surface (Figures 5B, 6C). Telotroch not observed.

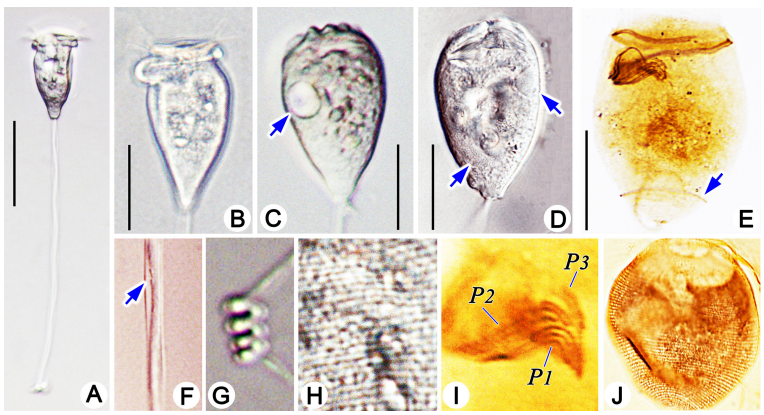

FIGURE 4
Photomicrographs of *Pseudovorticella dalianensis* sp. n. *in vivo* **(A–D, F–H)**, after protargol staining **(E, I)** and after silver nitrate staining **(J)**. **(A)** A typical complete individual. **(B)** A typical zooid. **(C)** Arrow marks a contractile vacuole. **(D)** Arrows point to a macronucleus. **(E)** Overview of the ciliature; arrow marks the aboral trochal band. **(F)** Details of the stalk and spasmoneme; arrow indicates granules. **(G)** Helically contracted stalk. **(H)** Pellicular striations. **(I)** Arrangement of infundibular polykineties. **(J)** Overview of the silverline system. P1–3, infundibular polykinety 1–3. Scale bars: 60 μm **(A)** and 30 μm **(B–E)**.

Haplokinety and polykinety circles extending about 1.25 turns around the peristomial disc and another turn after entering the infundibulum (Figure 5F, 6J). Polykinety posteriorly separated into three infundibular polykineties (P1, P2, and P3) at the lower half of the infundibulum (Figure 5F). Each infundibular polykinety consisting of three rows (Figures 5F, G). P2 terminating at the confluence of P1 and the outer rows of P3. In P3, the inner row shorter than the outer two rows and terminating at the same level as P2; the outer two rows parallel and equal in length, both beginning at the middle of the inner row; the outer two rows converged adstomally at the end of infundibulum, and terminating synchronously with P1 (Figures 5G, 6K). Germinal kinety located at the upper half of the infundibulum and parallel to haplokinety. Epistomial membrane located within the opening of the infundibulum (Figure 5G). The aboral trochal band composed of a row of kinetosomes encircling a cell at the posterior one-fourth of the body (Figures 5H, 6J).

Silverline system reticulate, with evenly spaced transverse lines (Figure 6L). 22–39 silverlines between the peristome and the trochal band, and 13–20 silverlines between the trochal band and the scopula (Table 1).

Phylogenetic analyses based on SSU rDNA sequences

The newly sequenced SSU rDNA of the three *Pseudovorticella* species in the present work, *P. zhejiangensis* sp. n., *P. dalianensis* sp. n., and *P. verrucosa*, have been deposited in the GenBank database with the accession numbers of OP216729 (partial length, 1,686 bp), OP216730 (partial length, 1,689 bp), and OP216731 (partial length, 1,600 bp), respectively. The GC contents of *P. zhejiangensis* sp. n., *P. dalianensis* sp. n., and *P. verrucosa* are 42.82%, 43.81%, and 43.87%, respectively.

The topologies of the phylogenetic trees constructed with RAxML, IQ-Tree, and MrBayes were highly identical; therefore, they were incorporated into one based on the topology of the RAxML tree (Figure 7). In the phylogenetic tree, the genus *Pseudovorticella* is non-monophyletic. Two distinct clades (marked as groups A and B) comprising the species of *Pseudovorticella* and *Epicarchesium* are identified. Group A contains *P. monilata*, *E. pectinatum*, and seven unclassified *Pseudovorticella* sequences, while group B contains all the remaining sequences of the genera *Pseudovorticella* and *Epicarchesium*, forming a sister cluster to one clade of *Vorticella* species. In group B, *P. zhejiangensis* sp. n. is clustered with two undefined isolates, *Pseudovorticella* sp.2 PERI98 (MW046187) and *Pseudovorticella* sp.2 PERI99 (MW046188) with full support values. *Pseudovorticella dalianensis* sp. n. is sister to *Pseudovorticella* sp. Dazhou bridge (KU363283) with full support values. They further cluster with *Epicarchesium corlissi* with high support values (99% in RAxML, 100% in IQ-Tree, and 1.00 in BI). *Pseudovorticella verrucosa* is sister to the clade of *P. sinensis* (DQ845295) and *P. parakenti* (MH537102) with support of 0.98 in BI (Figure 7).

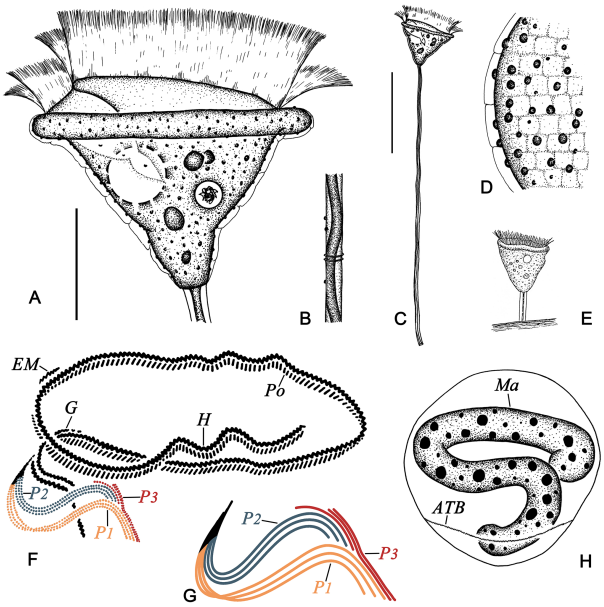

FIGURE 5
Pseudovorticella verrucosa from life **(A–E)** and after protargol staining **(F–H)**. **(A)** Typical shape of the zooid. **(B)** Details of the stalk and spasmoneme. **(C)** A complete individual with stalk and zooid. **(D)** Details of the pellicle. **(E)** The original illustration from Dons (1915). **(F)** Oral ciliature. **(G)** Arrangement of the three infundibular polykineties. **(H)** The macronucleus. ATB, aboral trochal band; EM, epistomial membrane; G, germinal kinety; H, haplokinety; Ma, macronucleus; Po, polykinety; P1–3, infundibular polykinety 1–3. Scale bars: 20 μm **(A)** and 70 μm **(C)**.

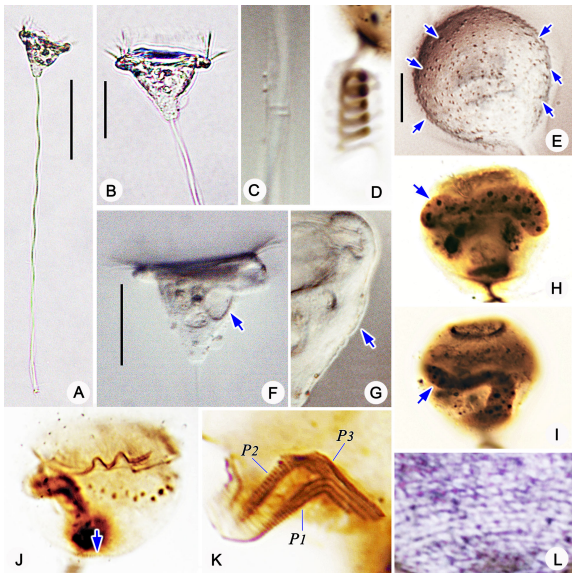

FIGURE 6
Photomicrographs of *Pseudovorticella verrucosa in vivo* **(A–C, E–G)**, after protargol staining **(H–K)** and after silver nitrate staining **(L)**. **(A)** A typical complete individual. **(B)** Zooid in typical shape. **(C)** Details of the stalk and spasmoneme. **(D)** Helically contracted stalk. **(E)** Pellicular granules (arrows). **(F)** Arrow marks the contractile vacuole. **(G)** Pellicular blisters (arrow). **(H–I)** Arrows point to the macronucleus. **(J)** Overview of the ciliature; arrow marks the aboral trochal band. **(K)** Infundibular part of the oral ciliature, showing the three polykineties. **(L)** Partial silverline system. P1–3, infundibular polykinety 1–3. Scale bars: 70 μm **(A)**, 30 μm **(B, E)**, and 10 μm **(D)**.

The genetic distances were calculated with MEGA7 among 25 *Pseudovorticella* sequences in group B (Table 2). The results showed that genetic distances differ from 0% to 7.01% between *P. zhejiangensis* sp. n. and other sequences, from 0.69% to 6.60% between *P. dalianensis* sp. n. and others, and from 1.71% to 6.74% between *P. verrucosa* and others. The sequence of *P. zhejiangensis* sp. n. is identical to *Pseudovorticella* sp.2 PERI99 (MW046188) and has only a generic distance of 0.07% to *Pseudovorticella* sp.2 PERI98 (MW046187). The sequences of *P. dalianensis* sp. n. and *Pseudovorticella* sp. Dazhou bridge (KU363283) share a generic distance of 0.69%. The sequence with the closest generic distance (1.71%) to *P. verrucosa* is *P. paracratera* (DQ662847).

Discussion

Brief review of the genus *Pseudovorticella*

Pseudovorticella Foissner & Schiffmann, 1975 is closely related to *Vorticella* Linnaeus, 1767, both of which are characterized by a solitary zooid borne upon a contractile stalk (Foissner and Schiffmann, 1975). The only difference between them is that the genus *Pseudovorticella* possesses a reticulate (*vs.* transverse) silverline system. The main distinguishing characters for *Pseudovorticella* species include 1) the shape and size of zooid, 2) the number and location of contractile vacuole(s), 3) the shape and position of macronucleus, 4) the appearance of oral morphology *in vivo*, 5) the pattern of oral ciliature, and 6) habitat (Warren, 1987; Song and Wilbert, 1989; Ji et al., 2003; Sun et al., 2009). The three species in the present work are compared below with their closely related species or populations.

Comparison of *Pseudovorticella zhejiangensis* sp. n. with related species

Pseudovorticella zhejiangensis sp. n. can be easily distinguished from most of its congeners by the number and location of contractile vacuoles (two with one ventral and one dorsal). However, four *Pseudovorticella* congeners, *P. jiangi* Sun et al., 2006, *P. jaerae* (Precht, 1935) Sun et al., 2009, *P. jankowskii* Sun et al., 2009, and *P. bidulphiae* (Stiller, 1939) Ji et al., 2009, and one *Vorticella* species, *V. picta* Ehrenberg, 1838, need to be compared with the new species owing to their similarity in gross morphology or the presence of pellicular blisters (Table 3).

Pseudovorticella jiangi and *P. jaerae* are similar to *P. zhejiangensis* sp. n. by several morphological characters (Table 3). However, *P. jiangi* differs from the new species by its larger zooid size *in vivo* (75–90 × 55–65 *vs.* 50–70 × 45–70 μm) and fewer silverlines above the aboral trochal band (20–24 *vs.* 31–38). *Pseudovorticella jaerae* has a slightly smaller body size (40–55 × 25–45 μm *vs.* 50–70 × 45–70 μm) and also fewer

silverlines above the aboral trochal band (20–26 *vs.* 31–38) than *P. zhejiangensis* sp. n. More importantly, both of the two known species have only one contractile vacuole (*vs.* two in the new species) (Precht, 1935; Sun et al., 2006; Sun et al., 2009).

Pseudovorticella jankowskii was reported to have two contractile vacuoles located near the ventral wall of the infundibulum, but it was shown as one ventral and one dorsal in its illustration (Sun et al., 2009). For this discrepancy, further study is needed. Nevertheless, apart from this character, it can be distinguished from the new species a slightly smaller body size *in vivo* (40–50 × 40–45 *vs.* 50–70 × 45–70 μm) and more silverlines below the aboral trochal band (20–23 *vs.* 9–17) (Sun et al., 2009).

Pseudovorticella bidulphiae has similar numbers of contractile vacuoles and silverlines with the new species (Table 3). However, *P. bidulphiae* can be separated from the new species by its smaller body size (30–40 × 35–40 *vs.* 50–70 × 45–70 μm), the absence of pellicular blisters (*vs.* presence), and a different structure of P3 (two-rowed *vs.* three-rowed) (Sun et al., 2009; Ji et al., 2011).

Pseudovorticella zhejiangensis sp. n. also resembles *Vorticella picta* in body shape and the number of contractile vacuoles. However, these two species can be clearly separated because the latter has a transverse silverline pattern (*vs.* reticulate), which is a key generic difference. In addition, *V. picta* was isolated from freshwater habitat (*vs.* brackish water) (Table 3) (Song and Wilbert, 1989).

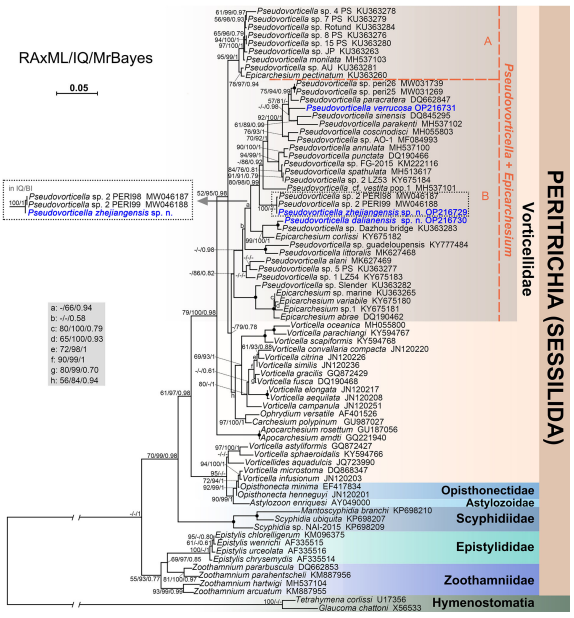

FIGURE 7
Phylogenetic tree of peritrich ciliates based on SSU rDNA sequences. Newly sequenced species are highlighted in blue. Numbers at the nodes represent support values in the following order: RAxML bootstrap values/IQ-Tree ultrafast bootstrap values/Bayesian inference (BI) posterior probabilities. "–" represent values below 50% or 0.50. Solid dots at the branching point indicate full support from all algorithms (100%/100%/1.00). The scale bar indicates five substitutions per 100 nucleotide positions.

Comparison of *Pseudovorticella dalianensis* sp. n. with related species

Pseudovorticella dalianensis sp. n. is characterized mainly by its distinctive arrangement of the rows in P3, i.e., the middle row is the longest. Five *Pseudovorticella* species, *P. longa* Song, 1997, *P. alani* Zhang et al., 2019, *P. elongata* (Fromentel, 1876) Leitner and Foissner, 1997, *P. sphagni* Foissner & Schiffmann, 1975, and *P. apogracilis* Sun et al., 2009, and a *Vorticella* species, *V. paralima* Liang et al., 2019, resemble the new species, and thus should be compared with the latter in detail (Table 3).

Pseudovorticella longa is highly similar to *P. dalianensis* sp. n. in terms of body shape, appearance of the peristomial lip, and the numbers of silverlines. However, the former can be separated from the latter by its smaller body size *in vivo* (30–45 × 15–25 *vs.* 50–60 × 30–35 μm) and the position of the contractile vacuole (dorsal *vs.* ventral). More importantly, the outer row is the longest in *P. longa*, which differs from that of *P. dalianensis* sp. n. (the middle row is the longest) (Song, 1997).

Pseudovorticella alani is distinctly larger *in vivo* (70–90 × 50–65 *vs.* 50–60 × 30–35 μm) than the new species, and it has more silverlines both above (48–61 *vs.* 31–44) and below the trochal band (12–20 *vs.* 9–13). Additionally, *P. alani* possesses a different pattern of P3 from that of *P. dalianensis* sp. n. (outer two rows about equal in length and longer than the inner row *vs.* the middle row is the longest) (Zhang et al., 2019).

Considering the body shape and size *in vivo*, further comparisons should be made with *Pseudovorticella elongata*, *P. sphagni*, and *P. apogracilis*. *Pseudovorticella elongata* has conspicuously more silverlines above the aboral trochal band (51–66 *vs.* 31–44 in the new species) and a different habitat (freshwater *vs.* marine) (Leitner and Foissner, 1997). *Pseudovorticella sphagni* has fewer silverlines above the aboral trochal band (26–27 *vs.* 31–44), a freshwater habitat (*vs.* marine), and two contractile vacuoles (*vs.* only one in *P. dalianensis* sp. n.) (Foissner, 1979). *Pseudovorticella apogracilis* has a slightly larger body size *in vivo* (60–70 *vs.* 50–60 μm) and more silverlines below the aboral trochal band (25–29 *vs.* 9–13) than *P. dalianensis* sp. n. (Sun et al., 2009).

Pseudovorticella dalianensis sp. n. has a strong resemblance to *Vorticella paralima* in body shape, number of silverlines, and the arrangement of P3 (Table 3). However, in addition to the typical reticulate silverline pattern (*vs.* transverse in *V. paralima*), a slightly larger body size *in vivo* (50–60 × 30–35 *vs.* 35–50 × 20–30 μm) and a ventral (*vs.* dorsal) located contractile vacuole can clearly distinguish the new species from *V. paralima* (Liang et al., 2019).

Comparison of *Pseudovorticella verrucosa* (Dons, 1915) Sun et al., 2009 with related populations and species

Pseudovorticella verrucosa (Dons, 1915) Sun et al., 2009 was first isolated from the surface of a hydra (*Laomedea* sp.) and reported under the basionym *Vorticella verrucosa* Dons, 1915 (Dons, 1915). After nearly one century, this rare species was redescribed by Sun et al. (2009) with its silverline system disclosed. The reticulate silverlines indicated that they should be a member of the genus *Pseudovorticella*. According to the brief original description, its typical morphological characters include a bell-shaped zooid with the length of about 60 μm, one contractile vacuole, and many conspicuous pellicular granules. Our population matches with these features very well. However, according to the original description, this species has a very short stalk (about 40 μm long when fully stretched, shorter than the zooid) (Figure 5E). Meanwhile, our form has a stalk about five times the length of the zooid. In addition, our isolate is slightly smaller than the original population (30–50 μm in length *vs.* ca. 60 μm). However, the length of stalk is usually considered as a character varying between populations. Thus, our isolate should be identified as a population of *P. verrucosa*.

Our isolate corresponds very well with the population reported by Sun et al. (2009), which includes 1) the inverted triangular-shaped zooid, 2) a J-shaped macronucleus, 3) conspicuous pellicular blisters, 4) highly developed pellicular granules, 5) a single contractile vacuole, 6) the number of transverse silverlines, 7) the arrangement of P3, and 8) the length of the stalk (i.e., about four to five times the length of the zooid). The only morphological difference between these two populations is the width of zooid in which our isolate is slightly wider (50–65 *vs.* 30–40 μm) (Sun et al., 2009) (Table 3).

Only a few *Pseudovorticella* species have both pellicular blisters and pellicular granules. Given these features, only two species, *P. faurefremieti* Sun et al., 2007 and *P. jiangi* Sun et al., 2006, need to be

TABLE 2 Genetic distances among SSU rDNA sequences of *Pseudovorticella* species in group B in the phylogenetic tree.

	Sequence	1	2	3	4	5	6	7	8	9	10	11	12	13	14	15	16	17	18	19	20	21	22	23	24
1	***P. zhejiangensis***	–																							
2	***P. dalianensis***	3.16	–																						
3	***P. verrucosa***	3.15	4.73	–																					
4	*P. alani*	3.63	3.15	4.72	–																				
5	*P. annulata*	3.01	4.04	3.76	4.17	–																			
6	*P. cf. vestita*	3.08	3.77	3.90	3.83	3.35	–																		
7	*P. coscinodisci*	3.02	4.39	2.88	3.84	3.22	3.15	–																	
8	*P. littoralis*	4.18	4.46	4.52	3.70	4.38	3.97	3.77	–																
9	*P. paracratera*	3.01	4.39	**1.71**	4.11	3.49	3.29	2.19	4.25	–															
10	*P. parakenti*	3.87	4.35	3.11	4.15	2.83	3.11	2.65	4.16	2.45	–														
11	*P. punctata*	2.81	3.98	3.70	3.83	0.55	3.15	3.08	4.11	3.08	2.74	–													
12	*P. sinensis*	4.18	5.35	2.74	4.79	3.76	3.63	2.60	4.93	2.26	2.55	3.63	–												
13	*P. spathulata*	2.94	3.91	3.29	4.17	1.03	2.67	2.81	4.32	2.94	2.55	0.96	3.08	–											
14	*P.* sp. 1 LZ54	3.35	3.22	4.31	1.78	3.15	3.15	3.70	3.08	4.11	4.15	3.35	4.72	3.56	–										
15	*P.* sp. 2 LZ53	2.94	3.91	3.29	4.17	1.03	2.67	2.81	4.32	2.94	2.55	0.96	3.08	0.00	3.56	–									
16	*P.* sp. 5 PS	3.15	2.88	4.11	1.57	3.49	3.08	3.29	2.67	3.76	3.58	3.22	4.18	3.29	1.44	3.29	–								
17	*P.* sp. AO-1	2.72	4.17	1.76	4.32	2.64	3.44	1.20	4.41	1.60	3.30	2.72	2.80	2.40	3.76	2.40	3.76	–							
18	*P.* sp. Dazhou	2.95	**0.69**	4.73	3.35	4.18	3.90	4.39	4.73	4.45	4.53	4.11	5.41	4.11	3.49	4.11	3.15	4.24	–						
19	*P.* sp. FG-2015	2.87	3.77	3.22	4.10	0.96	2.80	2.95	4.25	3.01	2.55	0.89	3.15	0.14	3.49	0.14	3.29	2.48	3.97	–					
20	*P.* sp. guadeloupensis	7.01	6.60	6.74	4.98	7.00	5.65	5.79	3.50	6.33	8.38	6.33	7.14	6.73	4.85	6.73	4.45	7.33	7.14	6.59	–				
21	*P.* sp. Slender	3.77	3.84	4.59	3.01	3.77	3.84	4.46	3.50	4.18	4.35	3.56	4.93	3.77	2.47	3.77	2.81	4.33	4.11	3.70	5.40	–			
22	*P.* sp. 2 PERI98	**0.07**	3.15	3.15	3.79	3.00	3.08	3.15	4.30	3.08	3.91	2.79	4.29	2.86	3.44	2.86	3.22	2.70	2.93	2.79	6.88	3.80	–		
23	*P.* sp. 2 PERI99	**0.00**	3.16	3.08	3.80	2.94	3.08	3.08	4.30	3.01	3.92	2.72	4.23	2.79	3.44	2.79	3.23	2.62	2.94	2.72	7.00	3.80	0.00	–	
24	*P.* sp. peri25	3.04	4.13	1.74	4.05	3.04	3.18	1.88	4.13	0.94	2.55	2.89	2.31	2.39	3.69	2.39	3.47	1.20	4.34	2.53	6.47	4.27	3.04	3.04	–
25	*P.* sp. peri26	3.03	4.04	1.73	3.96	3.03	3.17	1.88	4.11	0.94	2.53	2.88	2.31	2.38	3.67	2.38	3.46	1.19	4.25	2.52	6.34	4.18	3.03	3.03	0.00

Species in bold font represent the sequences newly reported in the present work. Numbers in bold font represent the minimum values of the three species in the present work. All values are in %.

compared with *P. verrucosa* (Table 3). *Pseudovorticella faurefremieti* differs from *P. verrucosa* by its elongate-shaped zooid (*vs.* inverted triangular-shaped) and a larger size *in vivo* (85–95 × 45–50 *vs.* 30–50 × 50–65 μm) (Sun et al., 2007). *Pseudovorticella jiangi* can be distinguished from *P. verrucosa* by a larger size *in vivo* (75–90 × 55–65 *vs.* 30–50 × 50–65 μm) and fewer silverlines below the aboral trochal band (9–11 *vs.* 13–20) (Sun et al., 2006).

Considering the zooid shape and pellicle blisters, *P. jankowskii* Sun et al., 2009 and *P. jaerae* (Precht, 1935) Sun et al., 2009 should be compared with *P. verrucosa* (Table 3). *Pseudovorticella jankowskii* can be clearly separated from *P. verrucosa* by having two contractile vacuoles (*vs.* one) and the absence of pellicular granules (*vs.* presence) (Sun et al., 2009). *Pseudovorticella jaerae* has a smooth pellicle without pellicular granules, which is one of the characteristics that can be distinguished from *P. verrucosa*. The additional differences between *P. jaerae and P. verrucosa* are zooid size *in vivo* (40–55 × 25–45 *vs.* 30–50 × 50–65 μm) and the number of silverlines below the aboral trochal band (8–11 *vs.* 13–20) (Precht, 1935; Sun et al., 2009).

Phylogenetic analyses of the genus *Pseudovorticella*

Up to date, there have been only 11 *Pseudovorticella* SSU rDNA sequences having taxonomic entries to the species level and about 23 other sequences not identified according to species (Sun et al., 2016; Zhang et al., 2019). We update the dataset with further three SSU rDNA sequences in the present study. The phylogenetic analyses inferred from more sequences are congruent with previous studies and confirm the non-monophyly of *Pseudovorticella* (Sun et al., 2016; Jiang et al., 2019; Zhang et al., 2019). One strong supporting evidence is that species of the genus *Epicarchesium* Jankowski, 1985 are aggregated with *Pseudovorticella* species (Li et al., 2008; Ji et al., 2015; Gómez et al., 2018), indicating their close relationship. Another piece of evidence is the robust relationship between *Pseudovorticella* and *Vorticella* species. In particular, group B comprising *Pseudovorticella* and *Epicarchesium* species is sister to one clade of *Vorticella*, which is consistent with the results reported by Sun et al. (2016).

TABLE 3 Morphological comparison of *Pseudovorticella zhejiangensis* sp. n., *Pseudovorticella dalianensis* sp. n., and *Pseudovorticella verrucosa* with their closely related taxa.

Species	Zooid size *in vivo* (μm)	Number of silverlines		Number, position of CV	Structure of P3	Habitat	Data source
		Above the ATB	Below the ATB				
***P. zhejiangensis* sp. n.**	50–70 × 45–70	31–38	9–17	2, ventral and dorsal	3-rowed	Brackish water	Present work
***P. dalianensis* sp. n.**	50–60 × 30–35	31–44	9–13	1, ventral	3-rowed	Marine	Present work
P. verrucosa	30–50 × 50–65	22–39	13–20	1, ventral	3-rowed	Brackish water	Present work
P. alani	70–90 × 50–65	48–61	12–20	1, ventral	3-rowed	Brackish water	Zhang et al. (2019)
P. apogracilis	60–70 × 30–40	39–44	25–29	1, ventral	3-rowed	Marine	Sun et al. (2009)
P. bidulphiae	30–40 × 35–40	25–31	9–13	2, ventral	2-rowed	Marine	Sun et al. (2009)
P. elongata	48–92 × 32–44	51–66	10–20	1, ventral	3-rowed	Freshwater	Leitner and Foissner (1997)
P. faurefremieti	85–95 × 45–50	30–33	15–18	1, ventral	3-rowed	Marine	Sun et al. (2009)
P. jaerae	40–55 × 25–45	20–26	8–11	1, ventral	3-rowed	Marine	Sun et al. (2009)
P. jankowskii	40–50 × 40–45	30–36	20–23	2, ventral	3-rowed	Marine	Sun et al. (2009)
P. jiangi	75–90 × 55–65	20–24	9–11	1, ventral	3-rowed	Marine	Sun et al. (2006)
P. longa	30–45 × 15–25	42–47	10–12	1, dorsal	3-rowed	Marine	Song (1997)
P. sphagni	40–50	26–27	8–10	2, ventral and dorsal	–	Freshwater	Foissner (1979)
P. verrucosa	40–50 × 30–40	33–37	17–21	1, ventral	3-rowed	Marine	Sun et al. (2009)
V. paralima	35–50 × 20–30	26–35	7–13	1, dorsal	3-rowed	Brackish water	Liang et al. (2019)
V. picta	35–55	35–46	22–27	2, –	–	Freshwater	Song and Wilbert (1989)

"–" represents data not available.
ATB, aboral trochal band; CV, contractile vacuoles; P3, polykinety 3.

The phylogenetic positions confirm the generic assignment of the three *Pseudovorticella* species. *Pseudovorticella zhejiangensis* sp. n. and *P. verrucosa* possess conspicuous pellicular blisters. They are clustered in group B containing *Pseudovorticella* cf. *vestita* pop.1 and *P. sinensis*, both having pellicular blisters (Ji et al., 2003; Jiang et al., 2019). However, most of the species in this clade, i.e., *P. paracratera*, *P. parakenti*, *P. coscinodisci*, *P. annulate*, *P. punctate*, and *P. spathulate*, do not possess pellicular blisters. Thus, it appears that the presence of pellicular blisters does not contain a phylogenetic signal among *Pseudovorticella* species.

By sequence comparison, the sequence of *Pseudovorticella zhejiangensis* sp. n. is identical to *Pseudovorticella* sp.2 PERI99 (MW046188) and has only a generic distance of 0.07% to *Pseudovorticella* sp.2 PERI98 (MW046187), and together with the close relationships to *P. zhejiangensis* sp. n. in the phylogenetic trees, these two unidentified sequences may represent populations of *P. zhejiangensis* sp. n.

Data availability statement

The data presented in the study are deposited in the NCBI repository with accession numbers OP216729, OP216730, and OP216731.

Author contributions

XL designed and supervised the study. MJ and ZS performed live observation and silver staining; YY drew the illustrations. YZ analyzed data, conducted species identification, and drafted the manuscript. ZQ, JL, and XL revised the manuscript. All authors contributed to the article and approved the submitted version.

Funding

This work was supported by the National Natural Science Foundation of China (42076113 and 42176145) and the Fundamental Research Funds for the Central Universities (20720200106 and 20720200109).

Conflict of interest

The authors declare that the research was conducted in the absence of any commercial or financial relationships that could be construed as a potential conflict of interest.

Publisher's note

Supplementary material

The Supplementary Material for this article can be found online at: https://www.frontiersin.org/articles/10.3389/fmars.2022.1030519/full#supplementary-material

SUPPLEMENTARY MATERIAL S1
Input file of RAxML and IQ-Tree.

SUPPLEMENTARY MATERIAL S2
Input file MrBayes.

SUPPLEMENTARY MATERIAL S3
The tree file of RAxML.

SUPPLEMENTARY MATERIAL S4
The tree file of IQ-Tree.

SUPPLEMENTARY MATERIAL S5
The log file of IQ-Tree.

SUPPLEMENTARY MATERIAL S6
The tree file of MrBayes.

SUPPLEMENTARY MATERIAL S7
The log file of MrBayes.

SUPPLEMENTARY MATERIAL S8
The output of jModeltest.

References

Berger, H., and Foissner, W. (2003). "Biologische methoden der gewässeranalysen: Ciliaten III-2.1. illustrated guide and ecological notes to ciliate indicator species (Protozoa, ciliophora) in running waters, lakes, and sewage plants," in *Handbuch angewandte limnologie: Grundlagen gewässerbelastung - restaurierung - aquatische Ökotoxikologie - bewertung - gewässerschutz*. Eds. C. Steinberg, W. Calmano, H. Klapper and R.-D. Wilken (Weinheim, Germany: Wiley-VCH Verlag GmbH & Co KgaA), 1–160. doi: 10.1002/9783527678488.hbal2003005

Chen, X., Li, Z., Hu, X., and Kusuoka, Y. (2010). Morphology, morphogenesis and gene sequence of a freshwater ciliate, *Pseudourostyla cristata* (Ciliophora, urostyloidea) from the ancient lake biwa, Japan. *Eur. J. Protistol.* 46, 43–60. doi: 10.1016/j.ejop.2009.08.002

Clamp, J. C. (2006). Redescription of *Lagenophrys cochinensis* santhakumari & gopalan 1980 (Ciliophora, peritrichia, lagenophryidae), an ectosymbiont of marine isopods, including new information on morphology, geographic distribution, and intraspecific variation. *J. Eukaryot. Microbiol.* 53, 58–64. doi: 10.1111/j.1550-7408.2005.00074.x

Darriba, D., Taboada, G. L., Doallo, R., and Posada, D. (2012). jModelTest 2: more models, new heuristics and parallel computing. *Nat. Methods* 9, 772. doi: 10.1038/nmeth.2109

Dons, C. (1915). Neue marine ciliaten und suctorien. *Tromsø Mus. Aarsh.* 38, 75–100.

Foissner, W. (1979). Peritriche ciliaten (Protozoa: Ciliophora) aus alpinen kleingewässern. *Zool. Jb. Syst.* 106, 529–558.

Foissner, W. (2016). Protists as bioindicators in activated sludge: identification, ecology and future needs. *Eur. J. Protistol.* 55, 75–94. doi: 10.1016/j.ejop.2016.02.004

Foissner, W., Berger, H., and Kohmann, F. (1992). "Taxonomische und Ökologische revision der ciliaten des saprobiensystems-band II," in *Peritrichida. heterotrichida odontostomtida* (Munich: Informationsberichte des Bayer, Landesamtes für Wasserwirtsch).

Foissner, W., Blake, N., Klaus, W., Breiner, H.-W., and Stoeck, T. (2010). Morphological and molecular characterization of some peritrichs (Ciliophora: Peritrichida) from tank bromeliads, including two new genera: *Orborhabdostyla* and *Vorticellides*. *Acta Protozool.* 48, 291–319.

Foissner, W., and Schiffmann, H. (1975). Biometrische und morphologische untersuchungen über die variabilität von argyrophilen strukturen bei peritrichen ciliaten. *Protistologica* 11, 415–428.

Foissner, W., and Schiffmann, H. (1979). Morphologie und silberliniensystem von *Pseudovorticella sauwaldensis* nov. spec. und *Scyphidia physarum* lachmann 1856 (Ciliophora: Peritrichida). *Ber. Nat. Med. Ver. Salzburg* 3–4, 79–83.

Gao, F., Warren, A., Zhang, Q., Gong, J., Miao, M., Sun, P., et al. (2016). The all-data-based evolutionary hypothesis of ciliated protists with a revised classification of the phylum ciliophora (Eukaryota, alveolata). *Sci. Rep.* 6, 24874. doi: 10.1038/srep24874

Gómez, F., Wang, L., and Lin, S. (2018). Morphology and molecular phylogeny of peritrich ciliate epibionts on pelagic diatoms: *Vorticella oceanica* and *Pseudovorticella coscinodisci* sp. nov. ciliophora, peritrichia). *Protist* 169, 268–279. doi: 10.1016/j.protis.2018.03.003

Hall, T. A. (1999). BioEdit: a user-friendly biological sequence alignment editor and analysis program for windows 95/98/NT. *Nucleic Acids Symp. Ser.* 41, 95–98.

Hoang, D. T., Chernomor, O., von Haeseler, A., Minh, B. Q., and Vinh, L. S. (2018). UFBoot2: improving the ultrafast bootstrap approximation. *Mol. Biol. Evol.* 35, 518–522. doi: 10.1093/molbev/msx281

Hu, X., Lin, X., and Song, W. (2019). *Ciliates atlas: Species found in the south China Sea* (Beijing: Science Press). doi: 10.1007/978-981-13-5901-9

Irwin, N. A. T., and Lynn, D. H. (2015). Molecular phylogeny of mobilid and sessilid ciliates symbiotic in eastern pacific limpets (Mollusca: Patellogastropoda). *J. Eukaryot. Microbiol.* 62, 543–552. doi: 10.1111/jeu.12208

Jankowski, A. (1985). Life cycles and taxonomy of generic groups *Scyphidia*, *Heteropolaria*, *Zoothamnium* and *Cothurnia* (class peritricha). *Trudy Zool. Inst. Leningr.* 12, 74–100.

Jiang, M., Hu, T., Wang, Z., Liang, Z., Li, J., and Lin, X. (2019). Morphology and phylogeny of three *Pseudovorticella* species (Ciliophora: Peritrichia) from brackish waters of China. *J. Eukaryot. Microbiol.* 66, 869–881. doi: 10.1111/jeu.12738

Ji, D., Kim, J. H., Shazib, S. U., Sun, P., Li, L., and Shin, M. K. (2015). Two new species of *Zoothamnium* (Ciliophora, peritrichia) from Korea, with new observations of *Z. parahentscheli* sun et al. 2009. *J. Eukaryot. Microbiol.* 62, 505–518. doi: 10.1111/jeu.12205

Ji, D., Shin, M. K., Choi, J. K., Clamp, J. C., Al-Rasheid, K. A. S., and Song, W. (2011). Redescriptions of five species of marine peritrichs, *Zoothamnium plumula*, *Zoothamnium nii*, *Zoothamnium wang*, *Pseudovorticella bidulphiae*, and *Pseudovorticella marina* (Protista, ciliophora). *Zootaxa* 2930, 47–59. doi: 10.11646/zootaxa.2930.1.4

Ji, D., Song, W., and Al-Rasheid, K. A. S. (2003). Description of a marine peritrichous ciliate, *Pseudovorticella sinensis* n. sp. (Ciliophora, peritrichia) from China. *J. Eukaryot. Microbiol.* 50, 360–365. doi: 10.1111/j.1550-7408.2003.tb00149.x

Ji, D., Song, W., and Warren, A. (2004). *Pseudovorticella paracratera* n. sp., a new marine peritrich ciliate (Ciliophora: Peritrichida) from north China. *Hydrobiologia* 515, 49–57. doi: 10.1023/B:HYDR.0000027317.26498.6a

Leitner, A. R., and Foissner, W. (1997). Taxonomic characterization of *Epicarchesium granulatum* (Kellicott 1887) jankowski 1985 and *Pseudovorticella elongata* (Fromentel 1876) nov. comb., two peritrichs (Protozoa, ciliophora) from activated sludge. *Eur. J. Protistol.* 33, 13–29. doi: 10.1016/S0932-4739(97)80018-1

Liang, Z., Shen, Z., Zhang, Y., Ji, D., Li, J., Warren, A., et al. (2019). Morphology and phylogeny of four new *Vorticella* species (Ciliophora: Peritrichia) from coastal waters of southern China. *J. Eukaryot. Microbiol.* 66, 267–280. doi: 10.1111/jeu.12668

Li, L., Song, W., Warren, A., Shin, M. K., Chen, Z., Ji, D., et al. (2008). Reconsideration of the phylogenetic positions of five peritrich genera, *Vorticella*, *Pseudovorticella*, *Zoothamnopsis*, *Zoothamnium*, and *Epicarchesium* (Ciliophora, peritrichia, sessilida), based on small subunit rRNA gene sequences. *J. Eukaryot. Microbiol.* 55, 448–456. doi: 10.1111/j.1550-7408.2008.00351.x

Lynn, D. H. (2008). *The ciliated Protozoa: Characterization, classification, and guide to the literature. 3rd ed* (Dordrecht: Springer). doi: 10.1007/978-1-4020-8239-9

Medlin, L., Elwood, H. J., Stickel, S., and Sogin, M. L. (1988). The characterization of enzymatically amplified eukaryotic 16S-like rRNA-coding regions. *Gene* 71, 491–499. doi: 10.1016/0378-1119(88)90066-2

Miller, M. A., Pfeiffffer, W., and Schwartz, T. (2010). "Creating the CIPRES science gateway for inference of large phylogenetic trees," in *Paper presented at the 2010 Gateway Computing Environments Workshop (GCE)* (New Orleans, LA: IEEE). 1–8. doi: 10.1109/GCE.2010.5676129

Minh, B. Q., Schmidt, H. A., Chernomor, O., Schrempf, D., Woodhams, M. D., von Haeseler, A., et al. (2020). IQ-TREE 2: new models and efficient methods for phylogenetic inference in the genomic era. *Mol. Biol. Evol.* 37, 1530–1534. doi: 10.1093/molbev/msaa015

Noland, L. E., and Finley, H. E. (1931). Studies on the taxonomy of the genus *Vorticella*. *Trans. Am. Microsc. Soc* 50, 81–123. doi: 10.2307/3222280

Precht, H. (1935). Epizoen der kieler bucht. *Nova Acta Leopol.* 3, 405–474.

Ronquist, F., and Huelsenbeck, J. P. (2003). MrBayes 3: Bayesian phylogenetic inference under mixed models. *Bioinformatics* 19, 1572–1574. doi: 10.1093/bioinformatics/btg180

Song, W. (1991). Contribution to the commensal ciliates on *Penaeus orientalis*. i. (Ciliophora, peritrichida). *Period. Ocean Univ. Qingdao* 21, 119–128.

Song, W. (1997). A new genus and two new species of marine peritrichous ciliates (Protozoa, ciliophora, peritrichida) from qingdao, China. *Ophelia* 47, 203–214. doi: 10.1080/00785236.1997.10428671

Song, W., and Wilbert, N. (1989). Taxonomische untersuchungen an aufwuchsciliaten (Protozoa, ciliophora) im poppelsdorfer weiher, Bonn. *Lauterbornia* 3, 2–221.

Song, W., and Wilbert, N. (1995). "Benthische ciliaten des süsswassers," in *Praktikum der protozoologie*. Ed. R. Röttger (New York: Gustav Fischer), 156–168.

Stamatakis, A. (2014). RAxML version 8: a tool for phylogenetic analysis and post-analysis of large phylogenies. *Bioinformatics* 30, 1312–1313. doi: 10.1093/bioinformatics/btu033

Sun, P., Clamp, J. C., Xu, D., Huang, B., and Shin, M. K. (2016). An integrative approach to phylogeny reveals patterns of environmental distribution and novel evolutionary relationships in a major group of ciliates. *Sci. Rep.* 6, 21695. doi: 10.1038/srep21695

Sun, P., Ji, D., Warren, A., and Song, W. (2009). "Solitary sessilid peritrichs," in *Free-living ciliates in the bohai and yellow seas, China*. Eds. W. Song, A. Warren and X. Hu (Beijing: Science Press), 217–256.

Sun, P., Ma, H., Shin, M. K., and Alrasheid, K. A. (2013). Morphology of two new marine peritrich ciliates from yellow Sea, *Pseudovorticella dingi* nov. spec. and *P. wangi* nov. spec., with supplementary descriptions of *P. plicata*, *P. banatica* and *P. anomala* (Ciliophora, peritrichia). *Eur. J. Protistol.* 49, 467–476. doi: 10.1016/j.ejop.2012.10.001

Sun, P., Song, W., and Warren, A. (2006). Taxonomic characterization of two marine peritrichous ciliates, *Epicarchesium corlissi* n. sp. and *Pseudovorticella jiangi* n. sp. (Ciliophora: Peritrichia), from northern China. *Eur. J. Protistol.* 42, 281–289. doi: 10.1016/j.ejop.2006.07.004

Sun, P., Song, W., and Xu, D. (2007). Two new marine species of *Pseudovorticella* (Ciliophora, peritrichia) from qingdao, north China. *Acta Protozool.* 46, 55–64.

Warren, A. (1986). A revision of the genus *Vorticella* (Ciliophora: Peritrichida). *Bull. Br. Mus. Nat. Hist. (Zool.)* 50, 1–57.

Warren, A. (1987). A revision of the genus *Pseudovorticella* foissner & schiffman 1974 (Ciliophora: Peritrichida). *Bull. Br. Mus. Nat. Hist. (Zool.)* 52, 1–12. doi: 10.5962/p.18297

Wilbert, N. (1975). Eine verbesserte technik der protargolimprägnation für ciliaten. *Mikrokosmos* 64, 171–179.

Wu, T., Li, Y., Lu, B., Shen, Z., Song, W., and Warren, A. (2020). Morphology, taxonomy and molecular phylogeny of three marine peritrich ciliates, including two new species: *Zoothamnium apoarbuscula* n. sp. and *Z. apohentscheli* n. sp. (Protozoa, ciliophora, peritrichia). *Mar. Life Sci. Technol.* 2, 31–40. doi: 10.1007/s42995-020-00046-y

Wu, T., Li, Y., Zhang, T., Hou, J., Mu, C., Warren, A., et al. (2021). Morphology and molecular phylogeny of three *Epistylis* species found in freshwater habitats in

China, including the description of *E. foissneri* n. sp. (Ciliophora, peritrichia). *Eur. J. Protistol.* 78, 125767. doi: 10.1016/j.ejop.2021.125767

Xu, G., Zhong, X., Wang, Y., Warren, A., and Xu, H. (2014). A multivariate approach to the determination of an indicator species pool for community-based bioassessment of marine water quality. *Mar. pollut. Bull.* 87, 147–151. doi: 10.1016/j.marpolbul.2014.07.068

Zhang, Y., Shen, Z., Zhang, F., Yu, Y., Li, J., and Lin, X. (2019). Taxonomy and phylogeny of *Pseudovorticella littoralis* sp. n. and *P. alani* sp. n. (Ciliophora: Peritrichia) from coastal waters of southern China. *Eur. J. Protistol.* 71, 125635. doi: 10.1016/j.ejop.2019.125635

Zhan, Z., Xu, K., Warren, A., and Gong, Y. (2009). Reconsideration of phylogenetic relationships of the subclass peritrichia (Ciliophora, oligohymenophorea) based on small subunit ribosomal RNA gene sequences, with the establishment of a new subclass mobilia kahl 1933. *J. Eukaryot. Microbiol.* 56, 552–558. doi: 10.1111/j.1550-7408.2009.00435.x